

SUBJECT: Interaction between the LEM
Descent Engine Exhaust Gas
and the Lunar Surface Material
Case 330

FROM: J. A. Saxton

TM- 66-1021-1

FACILITY FORM 602
 (ACCESSION NUMBER) 39
 (PAGES) CR75374
 (NASA CR OR TMX OR AD NUMBER)
 (TYPE) 29
 (CODE) 30
 (CATEGORY)

A great deal of evidence exists indicating that the lunar surface is covered to an indeterminate depth by granular material, the physical properties of which can only be crudely estimated at this time (Reference 5). It is of interest, therefore, to consider in general terms the nature and extent of the transfiguration of the lunar surface and surrounding atmosphere which could result from the impingement of the LEM descent engine exhaust gas upon that surface.

Roberts (References 1 and 2) has developed an analytic framework to describe the gas-surface interaction, and the approximate validity of his findings has been supported by the experimental work of Stitt (Reference 3) and, more recently, by Land and Clark (Reference 4). He postulates a model for the exhaust flow field and develops on this basis the resulting shear stress profile on the lunar surface. Some generalized assumptions concerning the mechanism of surface erosion then enable the development of expressions for such quantities as the height of incipient erosion, the rate of dynamic shear erosion, and an approximate expression for the total eroded depth for a simple descent flight profile.

One aspect of the present investigation was the utilization of the expression given by Roberts for the rate of "dynamic" surface erosion to numerically establish erosion profiles for several landing maneuvers, including an assessment of the effect of lateral velocity. In addition, a study was made of the distance traversed beyond the shock wave by lunar particles subject to the large dynamic pressure of the gas flow field. The results of the latter indagation are pertinent, relative both to vehicle impact and dust cloud height.

2020223242526272829303112345678
FEB 1977
RECEIVED
NSA SRI
N79-73387

Unclas

00/91 12614

BELLCOMM, INC.

COVER SHEET FOR TECHNICAL MEMORANDUM

TITLE - Interaction between the LEM
Descent Engine Exhaust Gas
and the Lunar Surface Material

TM - 66-1021-1

FILING CASE NO(S) - 330

DATE - February 15, 1966

AUTHOR(S) - J. A. Saxton

FILING SUBJECT(S) - Erosion
(ASSIGNED BY AUTHOR(S) - LEM Landing


ABSTRACT

The general character of LEM exhaust gas impingement upon the lunar surface and the criteria for the occurrence and nature of the resulting surface erosion and dust cloud formation have been discussed by Roberts (References 1 and 2). Motivated by the earlier experimental work of Stitt (Reference 3), Roberts formulated a semi-quantitative set of equations describing the gas flow field, rate of surface erosion, and extent of possible visibility occultation due to the dust cloud.

The purpose of the current investigation was to evaluate two specific aspects of the erosion problem via a numerical study; the erosion process itself was assumed to be described satisfactorily by Roberts' equations. Of primary interest was the establishment of nominal erosion profiles as a function of the descent velocity-vector with lunar particle diameter as a parameter. The possibility of vehicular damage resulting from particle-vehicle impact was also assessed.

The results of this study indicate that the maximum erosion depths to be encountered in the vicinity of the landing pad contact sites, which are located approximately fourteen feet in radial distance from the nozzle center-line, are only a fraction of a foot for particle diameters of one-tenth inch or less. On this basis the maximum surface slope produced is less than five degrees.

The erosion profiles resulting from several combinations of vertical and horizontal components of descent velocity are included and discussed. It should be noted that the extent of erosion described herein is subject to any deficiencies present in Roberts' theory and that this theory should be subjected to additional experimental verification beyond that furnished by the initial investigation of Land and Clark (Reference 4).



DISTRIBUTIONCOMPLETE MEMORANDUM TO

CORRESPONDENCE FILES:

OFFICIAL FILE COPY

plus one white copy for each
additional case referenced

TECHNICAL LIBRARY (4)

NASA Hq

G. Callas, MA-2
P. E. Culbertson, MTL
J. H. Disher, ML
E. Z. Gray, MT
T. A. Keegan, MA-2
W. B. Taylor, MLA
J. H. Turnock, MA

MSC Houston

O. E. Maynard
W. G. McMullen
O. O. Ohlsson, Jr.
C. Perrine
H. M. Scott

MSFC Huntsville

R. G. Crawford
R. E. Lavender

Langley Research Center

V. H. Blanchard
L. V. Clark
L. J. Fisher
N. S. Land
J. L. McCarty
L. Roberts
M. C. Walton, Jr.

Bellcomm-Complete Memorandum to

G. M. Anderson
C. J. Byrne
J. S. Dohnanyi
J. P. Downs
W. W. Ennis
P. L. Havenstein
N. W. Hinnners
J. A. Hornbeck
B. T. Howard
D. B. James
B. Kaskey
P. R. Knaff
R. K. McFarland
J. Z. Menard
C. R. Moster
I. D. Nehama
G. T. Orrok
R. Y. Pei
T. L. Powers
I. M. Ross
R. R. Schreib
S. H. Schachne
R. V. Sperry
W. Strack
T. H. Thompson
J. M. Tschirgi
R. L. Wagner
Department 1023
All members, Department 1021
Library

Analytic Framework

The fundamental equation describing the rate of surface erosion as given by Roberts (Reference 1) is:

$$\frac{1}{2} a u \frac{dm}{dt} = \tau_o - \tau^* \quad (1)$$

where

a : a dimensionless average momentum of the entrained dust

u : gas flow velocity

m : surface mass per unit area

τ_o : local shear stress without surface erosion

τ^* : local shear stress with surface erosion

This equation is simply a momentum balance which equates the amount of momentum transferred to the particles, i.e., utilized in surface erosion, to the excess of the local shear stress over that value, τ^* , at which the surface particles are held in mechanical equilibrium. The key to utilization of the equation, of course, lies in the proper interpretation of the relevant variables. As indicated previously, Roberts has developed the requisite relationships to enable such an evaluation. His development will not be reiterated here; however, a listing of the specific expressions employed in this study is given in Appendix A. For details of the derivation the reader is referred to References 1 and 2.

This investigation was restricted to the case which Roberts terms "dynamic" surface erosion. This refers to the flow condition in which the lunar surface roughness exceeds the boundary layer thickness of the gas expanding beneath the shock wave. The surface shear forces are then of the order of the dynamic pressure of the free stream. Such an assumption was made both because it should yield maximum values for erosion depth and because the majority of the erosion takes place at the lower altitudes for which such an assumption should be valid. Under such flow conditions Equation (1) becomes:

$$\frac{a \sigma c u}{2} \cos \beta \frac{\partial y}{\partial t} = c_f \rho \frac{u^2}{2} - F_g (\cos \beta - \sin \beta \cot \alpha) - F_{coh} \quad (2)$$

where

- c_f : friction coefficient for surface shear
- ρ : local gas density
- σ : particle density
- c : volume concentration of the lunar particles
- β : local surface slope
- y : erosion depth
- F_g : static friction per unit area
- F_{coh} : cohesive friction per unit area
- θ : azimuthal angle measured from the jet center-line
- α : static angle of repose of cohesionless particles
- t : time

Using Equation (2) it is possible to determine the local erosion rates on the lunar surface as a function of nozzle exit-plane altitude above the surface. The total erosion at a given surface locale can then be established in terms of the LEM descent maneuver characteristics.

The general descent philosophy assumed in this study was that the LEM will descend rapidly to an altitude of forty feet, at which point the descent rate will be slowed to a nominal four ft/sec and descent continued till touchdown. The details of the descent to forty feet are relatively unimportant insofar as producing any significant variation in the erosion profiles developed, and for that reason only the terminal descent phase will be considered. It is assumed that in that phase the vertical descent rate can be controlled to within three ft/sec and that the horizontal velocity component will be four ft/sec or less.

A listing of the computer program generated to accomplish the numerical evaluation is given in Appendix B. This listing plus the equations given in Appendix A should enable the reader to trace through the numerical procedure adopted. It is a straightforward application of Roberts' equations with an indexing scheme incorporated in order to enable assessment of the influence of lateral motion. The calculation procedure is of itself slightly conservative since the erosion rate throughout a given time increment is assumed equal to its value at the end of that increment, i.e., at the lower nozzle altitude.

Physical Assumptions

This section will be concerned with a discussion of the physical assumptions made in the evaluation of Equation (2). The values used to specify the state of the LEM descent engine exhaust gas were obtained from the rocket nozzle design program of M. W. Cardullo (Reference 6) and are listed in Appendix C. The engine was assumed to be operating in a throttled condition as it approached the lunar surface.

The assumptions made concerning the physical properties of the lunar surface material were relatively conservative. A particle density of 2.0 g/cc was assumed. This compares to values of 2.8 - 3.0 g/cc for basaltic lava and 2.7 g/cc for quartz sand. The particle volume concentration was taken to be 60%, corresponding to an orthorhombic configuration. While volume concentrations as low as 10% have been proposed (Reference 8), such high porosities could not occur to significant depths without the existence of cohesive forces; and there is some evidence to indicate that cohesive forces are not predominant (Reference 9). In this regard, the results obtained with the above assumptions are easily modified to reflect different assumptions since the erosion rate, as given by Equation (2), is explicitly dependent upon both particle density and concentration. Thus, a surface with 10% particle concentration would erode six times as rapidly as the one with 60% concentration.

The static angle of repose of the lunar surface particles was assumed to be 32°. Roberts has proposed this value for non-cohesive particles (Reference 1) based upon experimental data on a variety of soils, e.g., granite rock, aluminum oxide. It was also experimentally discovered that at smaller particle diameters ($d \lesssim 10^{-5}$ ft), cohesive forces predominate over the friction forces and the apparent angle of repose increases significantly. Based upon the assumption that the cohesive forces are of Van der Waals character, Roberts suggested that $F_{coh} = A_{coh} d^{-3}$ where

$$A_{coh} = 5 \times 10^{-17} \text{ lb-ft.}$$

The range of particle sizes considered was based upon the approximate limits established by electromagnetic spectral observations of the lunar surface. An upper limit of approximately 10^{-2} feet diameter has been set by radiometric reflectance measurements (Reference 10), and a lower limit of approximately 10^{-4} feet is appropriate based on the assumption that no cohesive forces exist. Results were obtained, however, for the somewhat broader range of 10^{-1} to 10^{-6} feet particles. Since the larger particles erode most

rapidly due to their smaller ballistic coefficient, which results in less depletion of the energy of the flow field subsequent to erosion (smaller average momentum), this study will be concerned for the most part with an examination of the erosion profiles of the 0.1 foot particles.

Two further quantities must be specified to complete the interpretation of Equation (2); these are the quantities a and c_f which characterize the flow field. The relationship proposed by Roberts (Reference 1) for the local momentum fraction a is listed in Appendix A. A comparison with the numerical results presented by Grossman (Reference 7) for particle acceleration in the expanding flow field beneath a normal shock furnishes some support for Roberts' expression. For the skin friction coefficient c_f Roberts suggests the value 0.2 as being applicable to hemispherical protuberances in dynamic shear flow. A brief check with the literature (Reference 11) suggests that this value is relatively high (and hence conservative), but inasmuch as this parameter essentially represents a means of data adjustment, its ultimate specification must be dictated by experimental criteria. In the following section theoretical predictions based upon a skin friction coefficient of 0.2 are compared with experimental data of Land and Clark (Reference 4).

Results

Of first importance in an analytical study of this type is a comparison of predicted results with available experimental evidence. As mentioned previously, Land and Clark have gathered experimental data on erosion profile development in several soils maintained in a moderate vacuum environment (10^{-4} torr) and impacted by a "cold-gas" (air at 530°R stagnation temperature) emerging from a one inch exit diameter conical nozzle. The general program developed to evaluate the lunar erosion profiles (Appendix B) was slightly modified to more closely model Land and Clark's experimental situation. The general calculational procedure takes into account the effect of the change of local surface slope on the shear and gravitational force components but neglects as second order the overall surface recession which occurs. The erosion depths achieved during the experimental measurements are of the order-of-magnitude of the original surface-to-nozzle distance, however, and for this reason the influence of surface recession was incorporated into the corresponding theoretical calculations.

Figure 1 represents a representative comparison between the experimental measurements and theoretical predictions. Some basic conclusions can be drawn regarding the interpretation of the theoretical curves. Good agreement with the experimental data has been achieved in the region of intermediate radial distances throughout the duration of the experiment, and for a short time interval, reasonable agreement occurs for all radial values; but as the experiment proceeds, an obvious breakdown in conformance can be perceived at both small and large radial distances. The deviation at the small radial values can be traced to a degeneracy in the numerical approximations made in the vicinity of the stagnation point, i.e., that point at which the gas velocity goes to zero and, consequently, no "theoretical" erosion takes place. The deviation at the larger radial distances indicates that the pressure distribution which describes the no-erosion situation is insufficient to fully characterize the flow conditions when erosion is occurring. The theoretical calculations do succeed, however, in the essential task of closely matching behavior in the vicinity of maximum "real" erosion, and for this reason it is felt that useful and relevant information can be gathered through numerical evaluation of Roberts' equations as applied to situations of current interest. Proceeding along this line of attack, then, the following results were obtained.

Figure 2 shows the maximum depth of the erosion profile incised upon the lunar surface as a function of particle size during a nominal terminal-descent maneuver, e.g., descent from a height of forty feet at constant descent velocity (four fps in this case). The maximum erosion which has occurred during the descent to five feet altitude is one foot or less for the range of particle sizes considered. During the descent to two feet altitude, which should be representative of the nozzle exit-plane altitude at landing-pad contact with the lunar surface, the calculational results indicate that the 0.1 foot particles are extremely rapidly eroded to a depth of several feet near the nozzle center-line. Roberts has pointed out, however, that the relationship appropriate for evaluating the surface pressure distribution when the nozzle is far from the surface over-estimates the pressure gradient directly beneath the nozzle at the lower nozzle altitudes. In addition, the basic nature of the isentropic expansion of the exhaust gas beneath the shock wave is altered if the surface in the vicinity of the stagnation point begins to erode into a cup-like cavity (cf. Figure 3). In the actual flow configuration the shock wave would be expected to dip only slightly into the cavity, with vortex motion arising within the cavity. The erosion process would then be related to the mechanism of vortex motion. Some of the flow field energy would be

diffused in the vortex motion itself, and a larger fraction of the remaining energy would be dissipated in fluid-particle interactions than in the flat surface case since the particles would tend to become momentarily entrained in the vortex motion. As a result, it seems reasonable to state that the extension of Roberts' formulation into the "near surface" regime leads to an over-estimation of the extent of erosion, and that localized hole-drilling would not occur (cf. Figure 1). Also, it is probable that the prime danger to be considered regarding operation of the LEM descent engine near the lunar surface is that of flow separation leading to nozzle rupture (Reference 12).

Since the erosion rate at a given height is independent of descent velocity, the results for two different descent velocities in cases of zero horizontal component can be directly compared on the basis of "exposure time", e.g., four times as much erosion occurs with a given particle size for a descent velocity of one fps as compared to four fps. Therefore, with a probable lowest descent velocity of one fps, the maximum erosion which would occur in a descent to five feet would be approximately four feet. In this case, the maximum erosion depth occurs at a radial distance of approximately two feet from the stagnation point. The flow should be subsonic at this point, and, therefore, a decreased flow velocity should be associated with the increased flow area created by the annular cavity formation. Thus, the "smooth surface" flow expansion assumption again over-estimates the magnitude of local shear and related erosion rate.

In addition, the largest erosion depths by a factor of five are attributable to the 0.1 foot diameter particles. As mentioned previously (cf. page 4), a more realistic upper limit for particle diameter is 0.01 foot. The maximum erosion depth occurring for particles of this size during a one fps vertical descent to five feet altitude is approximately one foot. In general, the results in this investigation are presented in terms of the 0.1 foot particles since this represents an upper limit and the results for other diameters are similar, except for the smaller particle diameters ($d < 10^{-5}$ ft) in which cohesive forces predominate. In this regard, the results for the 10^{-6} foot particles are not presented in Figure 2 since, if the cohesive force model proposed by Roberts is correct, no erosion has occurred in the descent to five feet and only negligible erosion occurs thereafter.

The manner in which the erosion profile develops during vertical descent is presented in Figure 3. The point of maximum erosion is seen to move steadily inward with decreasing height, and therefore, the landing conditions are milder than indicated in Figure 2 since the landing gear pads are located at a radial distance of fourteen feet, far from the point of maximum erosion. The salient feature of profile development is that the profile at any time is very much a function of the rate of erosion occurring at that time, and exhibits only at the larger radial distances the character of the previous erosion. One consequence of this aspect of surface removal is a reduction in the significance of the assumptions made with regard to the mechanism of erosion, e.g., specification of F_g , since the overall nature of the profile is determined by the erosion occurring when the nozzle is near the surface and for which $\tau_0 \gg \tau^*$.

Figure 4 presents a comparison of the erosion profiles which would be incised on the surface during a four ft/sec descent from forty feet to two feet nozzle height for three different horizontal velocities - 0, 2, and 4 fps, and Figure 5 gives the same information for a one ft/sec descent velocity. The profiles shown are centered at the point which is directly below the vehicle center-line when the nozzle exit-plane altitude equals two feet, which should approximately correspond to initial landing-pad contact with the lunar surface. It can readily be seen that a horizontal component of velocity has a slightly deleterious effect in terms of eroded depth at the landing-pad sites but does result in a smaller maximum eroded depth. One implication of the results which reflect the influence of lateral velocity is that an uphill landing would be least stable since the erosion process of itself creates an effective uphill slope with regard to vehicular motion. These calculational results are based upon an assumed initial ground-slope of zero, but qualitative considerations of mass flow velocity distribution suggest that a pre-existing uphill slope would further increase the rate of erosion behind the vehicle, whereas a downhill slope might be partially offset by the erosion.

A summation of the findings of this section is, then, that the erosion of lunar dust by the shear action of the LEM exhaust gas should not constitute a major hazard with regard to alteration of the LEM landing environment. The determining factors will be the relationship between the actual lunar soil properties and those assumed in these calculations and the mechanics of erosion at low nozzle-to-surface distances. Although the equations developed by Roberts and used in this investigation have received some experimental verification from the work of Land and Clark (Reference 4), it is imperative that additional experimental studies be conducted in order to furnish data in the low altitude regime to which Roberts'

theory cannot be applied. In any case, the optimum descent-profile for minimum erosion would be that which, subject to overall constraints, maximizes the descent velocity, employs minimum hover time near the surface, and minimizes the horizontal velocity component.

Particle Motion Above the Shock Wave

Subsequent to erosion the suspended dust particles are accelerated to some fraction of the expanding gas flow-field velocity as determined by the nature of the drag forces exerted. Nominally these particles should be accelerated in the radial direction only and should remain suppressed beneath the shock wave present at the surface. If, however, a particle strikes a protuberance of the lunar surface and is deflected upward through the shock wave, it enters a region of greatly increased dynamic pressure and it is the objective of this section to evaluate how far such a particle travels toward the vehicle before it is completely decelerated.

The geometry and vector notation employed is illustrated in Figure 6. In this coordinate system (two-dimensional) the particle's velocity and rate-of-change of velocity are given by:

$$\vec{V} = v_r \hat{e}_r + v_\theta \hat{e}_\theta \quad (3)$$

and

$$\frac{d\vec{v}}{dt} = \frac{dv_r}{dt} \hat{e}_r + \frac{dv_\theta}{dt} \hat{e}_\theta + v_r \frac{d\hat{e}_\theta}{dt} + v_\theta \frac{d\hat{e}_r}{dt} \quad (4)$$

where \hat{e}_r and \hat{e}_θ are unit vectors in the radial and azimuthal direction, respectively, and the last two terms in Equation (4) are related to coordinate rotation. The change in particle velocity is attributable solely to the drag force exerted upon the particle by the radial gas flow-field as given by:

$$\vec{F} = m \frac{d\vec{v}}{dt} = C_D A \frac{\rho}{2} (v_g - v_r)^2 \hat{e}_r \quad (5)$$

where

\vec{F} : drag force on the particle

m : particle mass

C_D : drag coefficient

A : particle cross-sectional area

ρ : gas density

v_g : gas velocity

v_r : particle velocity component in the radial direction

and the rate of coordinate rotation is defined as:

$$\frac{d\hat{e}_r}{dt} = \omega_\theta \hat{e}_\theta; \quad \frac{d\hat{e}_\theta}{dt} = -\omega_\theta \hat{e}_r \quad (6)$$

where

$$\omega_\theta = \frac{d\theta}{dt} = \frac{V_\theta}{r} \quad (7)$$

By substitution of Equations (4), (6), and (7) into Equation (5) the following two equations for particle motion in a radial gas flow-field result:

$$\frac{dv_\theta}{dt} = \frac{1}{r} V_\theta V_r \quad (8)$$

and

$$\frac{dv_r}{dt} = \frac{1}{r} V_\theta^2 + \frac{C_D A}{m} \frac{\rho}{2} (v_g - v_r)^2 \quad (9)$$

where ρ and v_g are functions of the azimuthal angle, θ .

Equation (8) can be solved in a straightforward manner, since $v_r = dr/dt$, leading to the result that

$$V_\theta = \omega_\theta r = -Kr \quad (10)$$

where K is a constant of integration. Physically, Equation (10) states that since there is no azimuthal component of drag force, the angular velocity, ω_θ , must remain constant. The equation of particle motion can now be obtained by substitution of Equation (10) into Equation (9)

$$\frac{dv_r}{dt} = K^2 r + \frac{\Delta}{2} \rho (v_g - v_r)^2 \quad (11)$$

where $\Delta = \frac{C_D A}{m}$ is the ballistic coefficient of the particle.

This equation is clearly nonlinear and must be solved numerically; however, a physically important special case can be discussed analytically. If a lunar particle were deflected upward directly toward the vehicle, it would have no azimuthal component of velocity, V_θ , and the resulting equation of motion would be:

$$\frac{dv_r}{dt} = \frac{\Delta}{2} \rho (v_g - v_r)^2 \quad (12)$$

Remembering that

$$\frac{dv_r}{dt} = \frac{dr}{dt} \frac{dv_r}{dr} = v_r \frac{dv_r}{dr} \quad (13)$$

Equation (12) can be written

$$\frac{v_r dv_r}{(v_g - v_r)^2} = \frac{\Delta}{2} \rho dr \quad (14)$$

Roberts assumes the velocity, V_g , to be a function only of θ and describes the density distribution of the LEM exhaust gas by

$$\frac{\rho}{\rho_n} = \frac{k}{2} (\cos\theta)^k \left(\frac{r_n}{r} \right)^2 \quad (15)$$

where:

ρ_n : gas density at the nozzle exit (one-dimensional flow assumption)

r_n : nozzle exit radius

k : flow parameter, function of engine operating conditions

r : radial distance from the nozzle.

If a constant supersonic drag coefficient is assumed, then, Equation (14) is equivalent to

$$\frac{V_r dv_r}{(v_g - v_r)^2} = K_1 \frac{dr}{r^2} \quad (16)$$

where

$$K_1 = \frac{\Delta}{2} \rho_n \frac{k}{2} r_n^2 (\cos\theta)^k = \text{constant} \quad (17)$$

and this can be integrated to

$$K_2 - \frac{K_1}{r} = \frac{1}{\frac{v_r}{1 - \frac{v_r}{v_g}}} + \log\left(1 - \frac{v_r}{v_g}\right) \quad (18)$$

where

$$K_2 = \frac{1}{\frac{(v_r)_o}{v_g} + 1} + \log\left(\frac{(v_r)_o}{v_g} + 1\right) + \frac{3}{4} \frac{C_D A}{\sigma dr_o} \quad (19)$$

and

$(V_r)_0$: initial upward particle velocity

σ : particle density

d : particle diameter

r_0 : initial radial particle location

The physical importance of Equation (18) is that it can be used to evaluate the possibility of vehicle impact by a particle which, having been radially accelerated by the gas stream beneath the shock wave, is deflected upward directly toward the vehicle. If we set $V_r = 0$, Equation (18) can be solved for the radial position at which a particle, having specified physical properties and an initial velocity, $(V_r)_0$, will have been completely decelerated.

The geometry of the situation considered is shown in Figure 7. The particle is assumed to have been eroded near the jet center-line and to have been accelerated a radial distance of seven feet (approximate radius of the LEM) and then deflected upward toward the center-point of the nozzle exit-plane. The values for the initial condition of upward particle velocity were obtained from a generalization of the results given by Grossman (Reference 6).

Figure 8 presents the general character of the results. Clearly, none of the particles come close to vehicular impact. The larger particles are decelerated more slowly due to their lesser ballistic coefficient, proportional to d^{-1} , and, therefore, travel further beyond the shock wave although possessing smaller initial velocity. Even the larger particles rise only a maximum distance of one foot above the shock wave, however, and in Figure 9 it is shown that this holds true for higher nozzle heights (vehicle altitude) as well. It should be noted that the larger particle diameters will correspond to the lower drag coefficient curve.

The dust cloud height beneath the vehicle is, thus, less than one foot higher than the shock wave, and Roberts' formula for the shock stand-off distance at the stagnation point yields for the LEM operating conditions:

$$S = 0.0577 h \quad (20)$$

where

S: shock stand-off distance

h: vehicle altitude

This expression has been shown to yield good agreement with the experimental data of Land and Clark (Reference 4) as illustrated in Figure 10. Thus, at a vehicle altitude of one hundred feet the dust cloud height should be about six feet and when the vehicle has descended to twenty feet the dust cloud should only be two feet high.

Such a tendency for "localization" of the dust cloud may be pertinent with regard to employment of the landing radar in that reflections from the top of the dust cloud immediately under the vehicle should represent a reasonably accurate measurement of altitude. Note, however, that the shock wave is spherical and, hence, the mechanism of shock wave entrapment does not seriously restrict dust cloud height at some distance to the side of the LEM. But it may be practical to employ a narrow beam height measuring radar aimed along the vehicle center-line.

Conclusions

The findings of this investigation suggest that the extent of surface erosion accompanying LEM descent engine exhaust-gas impingement upon the lunar surface will probably not be sufficient to create conditions which are hazardous to the lunar landing. That is, for particles of 0.1 inch diameter or less possessing physical properties similar to those assumed in these calculations, the predicted erosion depth at the landing-pad contact sites is only a fraction of one foot, even for the case of low velocity (one ft/sec) descent. The premise in this study was that though Roberts' analytical model is inapplicable near the jet center-line for low nozzle exit-plane to surface distances, it should over-estimate the situation in general and furnish a reasonable first estimate of the true situation at the larger radial distances at which the landing-pads are deployed. It is imperative, however, that additional experimental data on erosion be obtained in the "near surface" regime, e.g., nozzle exit-plane to surface distances of ten feet or less.

In regard to the possibility of vehicular damage by lunar ejecta impact, the dynamic pressure of the exhaust-gas flow serves as an effective suppressant for objects tending to move toward the vehicle. In fact, the dust cloud height should

be no more than one foot higher than the shock wave, even in the physically unlikely situation that the particles possess a sizeable initial velocity component toward the vehicle.


J. A. Saxton

1021-JAS-gdn

Attachments

References

Appendix A, B, and C

Figures 1-8

BELLCOMM, INC.

REFERENCES

1. "The Interaction of a Rocket Exhaust with the Lunar Surface", Leonard Roberts, NASA X64-90772, 1964.
2. "The Action of a Hypersonic Jet on a Dust Layer", Leonard Roberts, Inst. Aerospace Sci. Paper 63-50, January, 1963.
3. "Interaction of Highly Underexpanded Jets with Simulated Lunar Surfaces", Leonard Stitt, NASA TN D-1095, 1961.
4. "Experimental Investigation of Jet Impingement on Surfaces of Fine Particles in a Vacuum Environment", N. S. Land and L. V. Clark, NASA TN D-2633, 1965.
5. "Lunar Soil Mechanics, Landing Dynamics, and Apollo Site Survey", N. W. Hinners, Bellcomm TR-65-220-2, April 15, 1965.
6. "Design Program for Rocket Nozzles Based Upon Chemical Kinetics", M. W. Cardullo, Bellcomm TR-65-130-1, September, 1965.
7. "Characteristics of Particles Blown Away by Exhaust Jet Impingement on a Lunar Surface", R. L. Grossman, GAEC Report No. ADR 04-04062.3, December, 1962.
8. "Depth and Strength of the Lunar Dust", L. D. Jaffe, Trans Air, Geophys. Union 45 628, December, 1964.
9. "Lunar Surface Models", R. F. Fudali, Bellcomm Memorandum for File, February 15, 1965.
10. "Nature of the Surface of the Planets and of the Moon", A. Dollfus, NASA W-1143(23), 1959.
11. Boundary Layer Theory, H. Schlichting, McGraw-Hill Book Company, Inc. New York, 1960, pp. 551-557.
12. "Effects of Fly-In and Nozzle Crushing on the Abort Capability of the LEM Descent Engine", J. A. Nutant and J. Wong, Bellcomm Memorandum for File, December 13, 1965.

APPENDIX A

This appendix lists the relationships developed by Roberts which enable interpretation of Equation (1). For a more complete development the reader is referred to References 1 and 2. The equations are listed with a brief caption and are numbered to correspond to the equation numbers in References 1 and 2.

1. Overall momentum balance:

$$\frac{1}{2} a u \frac{dm}{dt} = \tau - \tau^* \quad (1-23)$$

where

a: non-dimensional particle momentum fraction

u: gas flow velocity

m: bulk lunar soil weight per unit area

t: time

τ : surface shear stress without erosion

τ^* : surface shear stress with erosion

2. Gas dynamic pressure distribution along the surface:

$$\frac{\rho u^2}{2} = \frac{2\gamma}{\gamma-1} \left[1 - \left(\frac{p}{p_s} \right)^{\frac{\gamma-1}{\gamma}} \right] \left(\frac{p}{p_s} \right)^{\frac{1}{\gamma}} p_s \quad (2-A15)$$

with

$$\frac{p}{p_s} = e^{-\xi^2}, \quad \xi^2 = \frac{k+4}{2} \tan^2 \theta \quad (1-4)$$

$$p_s = \frac{k+2}{2} \frac{F}{\pi h^2} \quad (1-6)$$

and

$$k = \gamma(\gamma-1) M_n^2 \quad (1-1)$$

where

ρ : local gas density

p : local static pressure

p_s : stagnation point pressure

F : vehicle thrust

h : nozzle exit plane altitude

γ : ratio of heat capacities

M_n : Mach number at nozzle exit

θ : azimuthal angle measured from the nozzle exit-plane

e : base of the natural logarithm system

3. Surface shear without erosion

$$\tau^* = F_g(\cos\beta - \sin\beta \cot\alpha) + F_{coh} \quad (1-18b)$$

with

$$F_{coh} = A_{coh}/d^3 \quad (1-20)$$

$$F_g = \sigma g d c \cdot \tan\alpha$$

where

β : angle of surface slope

α : static angle of repose of cohesionless particles

A_{coh} : cohesive force parameter

d : lunar particle diameter

BELLCOMM, INC.

Appendix A

- 3 -

- σ : particle density
 g : lunar gravitational acceleration
 c : volume concentration of lunar particle

4. Non-dimensional particle momentum factors:

$$a = \left[0.5 + \sqrt{0.25 + \xi^{-1}} \right]^{-1} \quad (1-26)$$

$$\zeta = \frac{18\mu_c h \sqrt{\frac{2}{k+4}}}{\sqrt{2} \sigma d^2 \sqrt{RT_c}} \left[1 + \frac{\sqrt{2} C_D}{72e} \frac{F}{\pi \left(h \sqrt{\frac{2}{k+4}} \right)^2} \frac{d}{\mu_c \sqrt{RT_c}} \right] \quad (1-27)$$

where

- a : non-dimensional particle momentum fraction
 μ_c, T_c : chamber gas viscosity and temperature
 C_D : particle drag coefficient

APPENDIX B

```
(JOB          JAS2,JAS,5330,1021
(DATA
$IBFTC LEROS  LIST
C
C TITLE       LUNAR DUST EROSION PROFILES
C
C AUTHOR      J.A. SAXTON
C
C PURPOSE     TO ESTABLISH THE EROSION PROFILE INCUSED UPON THE LUNAR
C              SURFACE BY THE LEM ROCKET EXHAUST DURING LUNAR LANDING.
C
C
C INPUT DATA
C
      DIMENSION D(6),CD(6),DELY(950),Y(950),
      R(950),SLOP(950),ANGL(950),DELH(10)
      CALL BLDID(2HHO,HO,2HHF,HF,5HVDESC,VDESC,4HVVHOR,VHOR)
      CALL BLDID(1HF,F,5HEXPAN,EXPAN,2HTO,TO)
      CALL BLDID(4HCVIS,CVIS,4HWMOL,WMOL)
      CALL BLDID(5HGAMMA,GAMMA,2HRSK,SK,2HRN,RN)
      CALL BLDID(1HG,G,5HSIGMA,SIGMA,4HCONC,CONC)
      CALL BLDID(5HALPHA,ALPHA,4HACOH,ACOH,2HCF,CF)
      CALL BLDID(4HDELX,DELX,3HINC,INC,3HSWT,SWT)
      CALL BLDAR(4HDELH,DELH,4)
      CALL BLDAR(2HCD,CD,6)
      CALL BLDAR(1HD,D,6)
      CALL READ
C
C INITIAL PRINT OUT
C
      WRITE(6,1000)
      WRITE(6,1500)F,EXPAN,TO
      WRITE(6,1540)CVIS,WMOL,GAMMA,SK,RN
      WRITE(6,1550)HO,HF
      WRITE(6,1560)G,TO,SIGMA
      WRITE(6,1570)CONC,ALPHA,ACOH,CF
      WRITE(6,1580)(CD(I),I=1,6)
      WRITE(6,1600)DELX,INC
      WRITE(6,1610)(DELH(I),I=1,4)
C
C GENERAL PARAMETERS
C
      RBAR=4.9686E04/WMOL
      SRT=SQRT(RBAR*TO)
      GAMRT=GAMMA/(GAMMA-1.)
      RT=2.*GAMRT*RBAR*TO
      E=(SK+4.)/GAMRT
      PFACT=F/3.1416*(SK/2.+1.)
      TANALP=SIN(ALPHA)/COS(ALPHA)
      KMAX=42./DELX+1.
      KL=1./DELX+1.
      KH=KMAX-KL+1
      GO TO 51
C
C SPECIFY TRAJECTORY
```

```

C
50      CALL READ
      IF(SWT.EQ.1.)CALL EXIT
51      DELR=VHOR/VDESC*(HO-HF)
      RL=DELR-21.
      DO 10 K=1,KMAX
      RK=K-1
10      R(K)=RL+RK*DELR
C
C SPECIFY PARTICLE DIAMETER
C
      DO 200 J=1,6
      T=0.
      H=HO
      RC=0.
      DO 20 K=1,KMAX
      Y(K)=0.
      ANGL(K)=0.
20      SLOP(K)=0.
C
C INITIATE CALCULATIONS
C
      DO 250 N=1,4
      DELT=DELH(N)/(10.*VDESC)
      DRC=DELT*VHOR
      DO 300 I=1,10
      T=T+DELT
      H=H-VDESC*DELT
      RC=RC+DRC
      HFACT=H*SQRT(2./(SK+4.))
      PS=PFACT/H**2
      Z1=12.73*HFACT/(SIGMA*D(J)**2*SRT)*CVIS
      Z2=2.30E-3*CD(J)*F/(HFACT**2*CVIS)*D(J)/SRT
      ZETA=Z1*(1.+Z2)
      A=1./(0.5+SQRT(0.25+1./ZETA))
      DO 400 K=1,KMAX
      IF(R(K).GE.RC)GO TO 35
      RAD=RC-R(K)
      ANGL(K)=-ANGL(K)
      GO TO 40
35      RAD=R(K)-RC
40      B=ATAN(RAD/H)
      IF(B.GT.0.7854)GO TO 400
      VEL=(RT*(1.-COS(B)**E))**.5
      XI=SQRT((SK+4.)/2.)*SIN(B)/COS(B)
      PRATIO=EXP(-XI**2)
      DYNHD=GAMRT*PS*(PRATIO**(1./GAMMA)-PRATIO)
      TAU=CF*DYNHD
      FCOH=ACOH/D(J)**3*32.2
      FGRAV=SIGMA*G*D(J)*CONC*TANALP
      TAUSTR=FGRAV*(COS(ANGL(K))-SIN(ANGL(K))/TANALP)+FCOH
      IF(TAU.LT.TAUSTR)GO TO 400
      DELY(K)=2./(SIGMA*CONC*A*VEL*COS(ANGL(K)))*(TAU-TAUSTR)
      *DELT
      Y(K)=Y(K)+DELY(K)

```

```

400      CONTINUE
        DO 550 K=1,KMAX
          SLOP(K)=SLOPE(Y,DELX,K,KMAX)
          ANGL(K)=ATAN(SLOP(K))
          CONTINUE
C
C      PRINT OUT
C
        WRITE(6,1999)VHOR
        WRITE(6,2000)D(J),A,T,H,VDESC
        WRITE(6,2001)
        WRITE(6,2002)(R(K),Y(K),SLOP(K),K=KL,KH,INC)
250      CONTINUE
200      CONTINUE
        GO TO 50
C
C FORMATS
C
1000      FORMAT(1H1////56X,22HLEMD EROSION PROFILES/
        .      54X 25HADVANCED SYSTEMS DIVISION/
        .      46X 41HVEHICLE ENGINEERING AND ADVANCED MISSIONS/
        .      61X 12HJ. A. SAXTON)
1500      FORMAT(///5X,17HENGINE PARAMETERS//
        .      10X,8HTHRUST= ,1PE9.3,13H LB*FT/SEC**2/
        .      10X,17HEXPANSION RATIO= ,0PF5.1/
        .      10X,15HCHAMBER TEMP.= ,F6.0,10H DEG.RANK.)
1540      FORMAT(10X,15HCHAMBER VISC.= ,1PE11.2,10H LB/FT/SEC/
        .      10X,15HEXIT MOL. WT.= ,0PF5.2/
        .      10X,7HGAMMA= ,F5.3/10X,3HK= ,F10.3/
        .      10X,15HNOZZLE RADIUS= ,F6.1,4H FT.)
1550      FORMAT(///5X,18HDESCENT TRAJECTORY//
        .      10X,16HINITIAL HEIGHT= ,F8.1,4H FT./
        .      10X,14HFINAL HEIGHT= ,F8.1,4H FT.)
1560      FORMAT(///5X,18HSURFACE PARAMETERS//
        .      10X,13HGRAV.ACCEL.= ,F7.3,10H FT/SEC**2/
        .      10X,18HSTAGNATION TEMP.= ,F6.0,10H DEG.RANK./
        .      10X,18HPARTICLE DENSITY= ,F4.0,9H LB/FT**3)
1570      FORMAT(10X,16HPARTICLE CONC.= ,F7.2/
        .      10X,17HANGLE OF REPOSE= ,F5.3,8H RADIANS/
        .      10X,17HCOHESION COEFF.= ,1PE11.1,6H LB*FT/
        .      10X,17HFRICITION COEFF.= ,0PF6.2)
1580      FORMAT(10X,14HDRAG COEFFS.= ,5(F6.2,2H, ),F6.2)
1600      FORMAT(///5X,20HINPUT-OUTPUT CONTROL//
        .      10X,18HMATRIX INCREMENT= ,F8.2/
        .      10X,21HPRINT OUT INCREMENT= ,I3)
1610      FORMAT(10X,18HHEIGHT INCREMENT= ,3(F8.2,2H, ),F8.2)
1999      FORMAT(1H1,5X,12HEROSION WITH,F4.1,22H FT. LATERAL VELOC
        .ITY)
2000      FORMAT(///5X,9HDIAMETER= 1PE12.3,4H FT./
        .      5X,19HMOMENTUM FRACTION= ,E12.3/
        .      5X,14HDESCENT TIME= 0PF9.2,6H SECS./5X,8HHEIGHT= F9.2,
        .      4H FT./5X,18HDESCENT VELOCITY= ,F7.2,7H FT/SEC)
2001      FORMAT(///5X,15HRADIAL LOCATION,5X,13HEROSION DEPTH,5X,
        .      19HCORRESPONDING SLOPE//)
2002      FORMAT(10X,0PF5.1,10X,1PE12.3,8X,E12.3)

```



```

                                END
$IBFTC SLOPE
C TITLE          LAGRANGIAN DIFFERENTIATION
C
C AUTHOR         JE HOLCOMB
C
C DATE          7/21/65
C
C PURPOSE       TO APPROXIMATE THE DERIVATIVE AT A GIVEN POINT
C
C METHOD        LAGRANGIAN FIVE POINT DIFFERENTIATION FORMULAS ARE USED
C              WITH SPECIAL FORMULAS FOR POINTS 1,2,N-1,AND N.
C              REFERENCE  FIRST COURSE IN NUMERICAL METHODS
C                        WALTER JENNINGS
C                        CHAPTER 13 PAGE 106
C
C NOTE         THIS ROUTINE DOES NOT HAVE ERROR-ANALYSIS FACILITIES,
C              THEREFORE IT IS NOT ADVISED FOR USE IN SITUATIONS WHERE
C              THE NATURE OF THE DERIVATIVE IS NOT KNOWN.  THE
C              ROUTINE IS NOT INTENDED TO BE GENERAL PURPOSE.
C
C CALL         FUNCTION SLOPE(Y,DX,I,IMAX)
C
C INPUT        VARIABLE      DESCRIPTION
C
C              Y              TABLE OF FUNCTION VALUES
C              DX             INCREMENT ON X-AXIS
C              I              SUBSCRIPT OF POINT AT WHICH SLOPE
C                           IS TO BE APPROXIMATED
C              IMAX           TOTAL NUMBER OF DATA POINTS
C
C OUTPUT
C              SLOPE          SLOPE AT DESIRED POINT
C
C              FUNCTION SLOPE(Y,DX,I,IMAX)
C
C              DIMENSION Y(1)
C
C              COMPUTE DIVISOR
C
C              H=12.*DX
C
C              TEST FOR POINT BEING 1,2,IMAX-1, OR IMAX
C
C              IF(((IMAX-I).LT.2).OR.(I.LT.3))GO TO 100
C
C              FOLLOWING FORMULA IS FOR 3.LE.I.LE.(IMAX-2)
C
C              SLOPE=(Y(I-2)-8.*Y(I-1)+8.*Y(I+1)-Y(I+2))/H
C              RETURN
C
C              TEST TO DETERMINE WHICH END OF TABLE
C
C 100          IF(I-2)200,300,400
C
```

C FOLLOWING FORMULA FOR I=1

C
200 SLOPE=(-25.*Y(I)+48.*Y(I+1)-36.*Y(I+2)+16.*Y(I+3)
-3.*Y(I+4))/H
RETURN

C
C FOLLOWING FORMULA FOR I=2

C
300 SLOPE=(-3.*Y(I-1)-10.*Y(I)+18.*Y(I+1)-6.*Y(I+2)+Y(I+3))/H
RETURN

C
C TEST TO DETERMINE WHETHER I=IMAX-1 OR I=IMAX

C
400 IF(I-IMAX+1)700,600,500

C
C FOLLOWING FORMULA FOR I=IMAX

C
500 SLOPE=(3.*Y(I-4)-16.*Y(I-3)+36.*Y(I-2)-48.*Y(I-1)
+25.*Y(I))/H
RETURN

C
C FOLLOWING FORMULA FOR I=IMAX-1

C
600 SLOPE=(-Y(I-3)+6.*Y(I-2)-18.*Y(I-1)+10.*Y(I)+3.*Y(I+1))/H
700 RETURN
END

\$ENTRY LEROS
HO=40.,HF=2.,VDESC=7.,VHOR=0.,
F=9.66F4,EXPAN=50.2,TO=5047.,
CVIS=4.E-5,WMOL=20.58,
GAMMA=1.329,SK=10.344,RN=2.,
G=5.31,SIGMA=125.,CONC=0.6,
ALPHA=0.559,ACOH=5.E-17,CF=0.2,
DETX=0.5,INC=1,SWT=0.,
DFLH=20.,10.,5.,3.,
D=1.E-1,1.E-2,1.E-3,1.E-4,1.E-5,1.E-6,
CD=1.05,1.25,1.86,5.0,23.5,82.0/
VHOR=2./
VHOR=4./
VDESC=4.,VHOR=0./
VHOR=2./
VHOR=4./
VDESC=1.,VHOR=0./
VHOR=2./
VHOR=4./
SWT=1./
(BATCH 10
(REMOVE ALL
(ENDJOB

BELLCOMM, INC.

APPENDIX C

The engine and nozzle operating conditions used in this investigation were obtained from a nozzle flow-analysis computer program developed by M. W. Cardullo (Reference 5). As the vehicle slowly approaches the lunar surface during the last stages of descent, the engine will be operating in a throttled condition which was assumed to correspond to a chamber pressure of 30 psia. From a Bray analysis the remaining nozzle and chamber parameters were ascertained to be:

1. Chamber:

$$T_o = 5047^\circ\text{R}$$

2. Nozzle Exit:

$$p_n = 0.0564 \text{ psia}$$

$$T_n = 1315^\circ\text{R}$$

$$MW = 20.58$$

$$C_p = 0.39 \text{ Btu/lb}^\circ\text{R}$$

$$\gamma = 1.329$$

$$M_n = 4.863$$

$$e = 50.177 \text{ (LEMDE: } e = 47.4)$$

$$R = 2414 \frac{\text{ft}^2}{\text{sec}^2 \text{ } ^\circ\text{R}}$$

3. General Performance:

$$I_{\text{vac}} = 320.2 \text{ sec}$$

$$F = 2983 \text{ lb.}$$

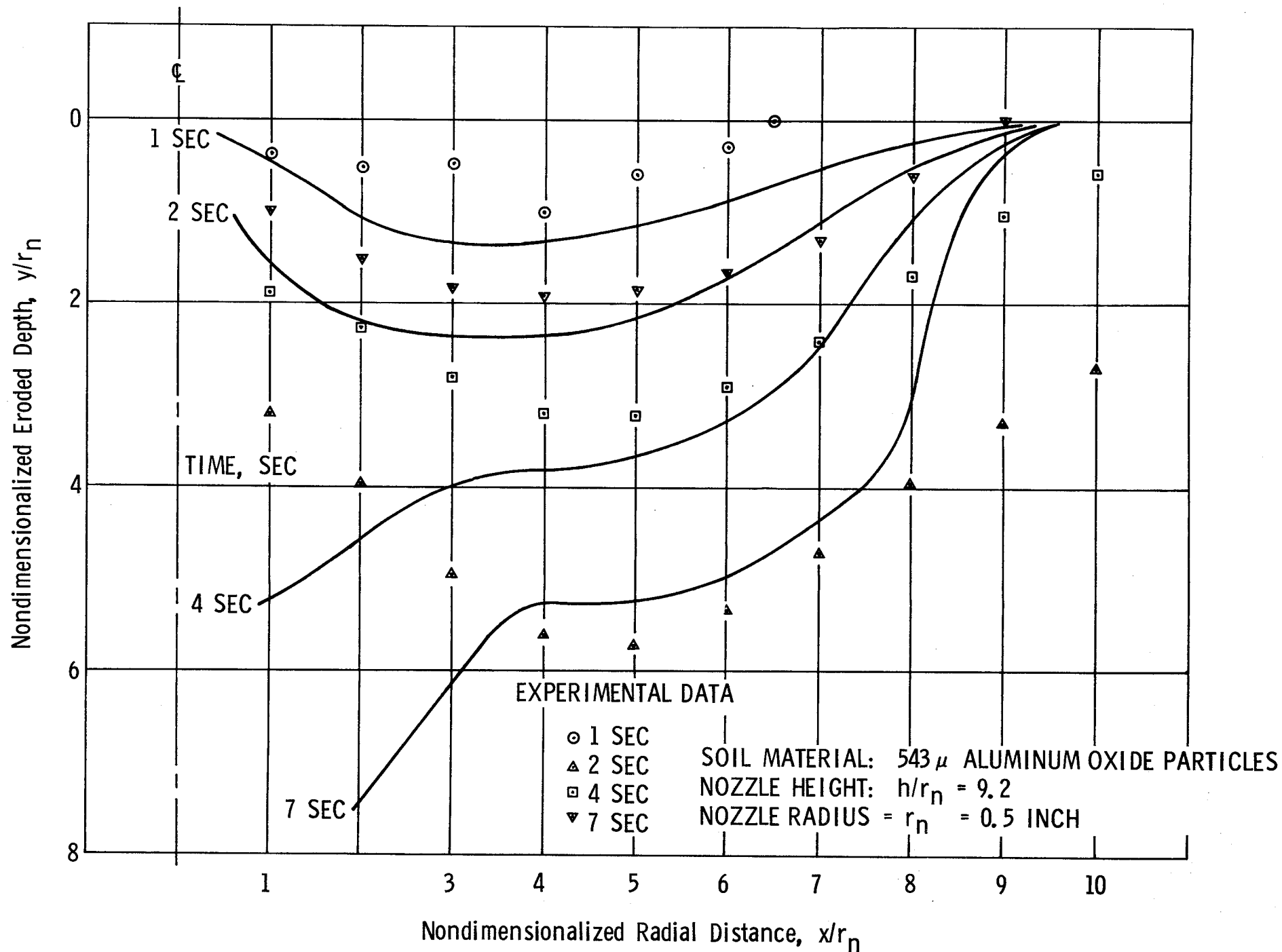


FIGURE 1 COMPARISON BETWEEN THEORETICAL EROSION PROFILES AND LAND AND CLARK'S EXPERIMENTAL DATA

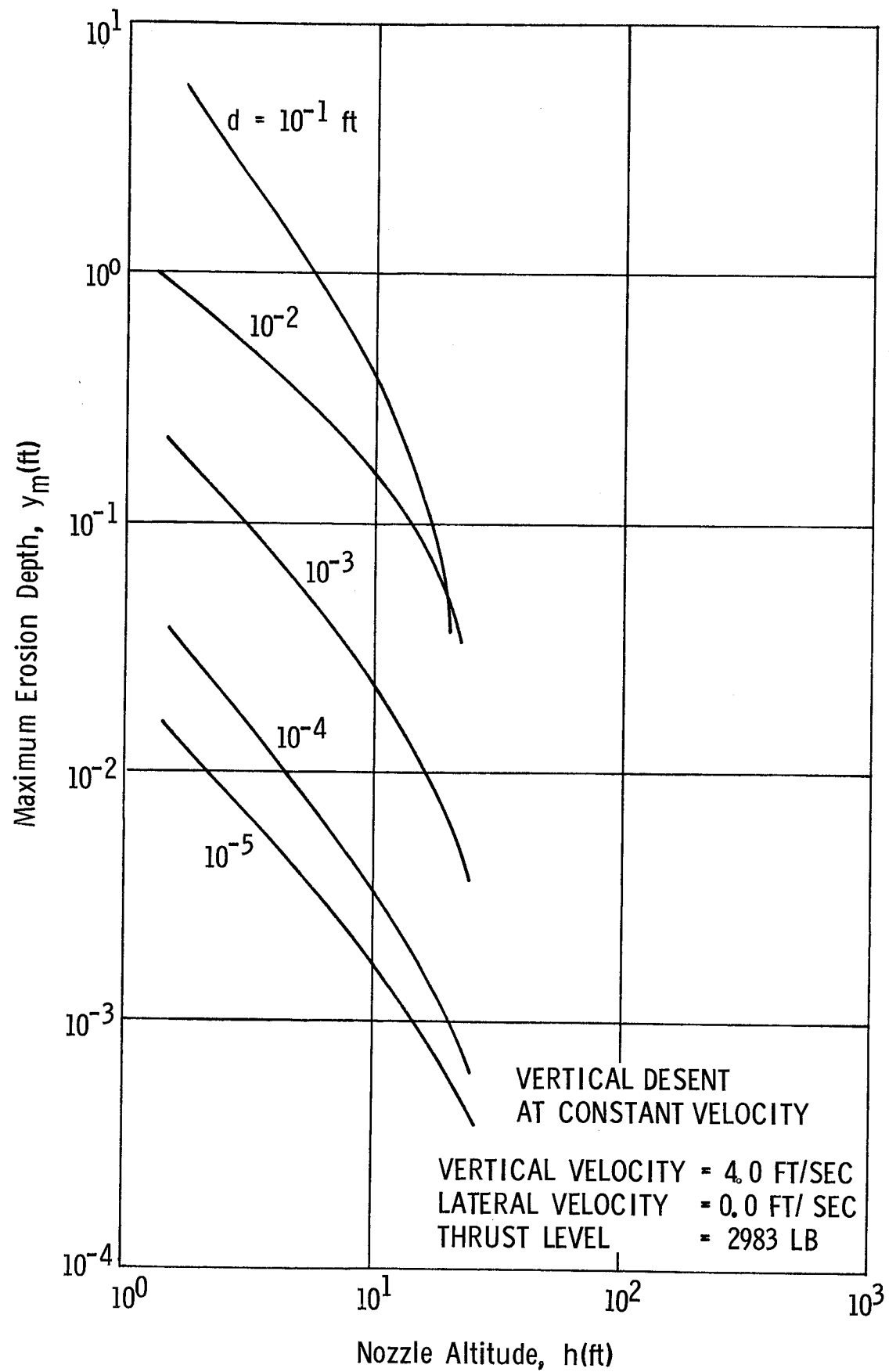


FIGURE 2 MAXIMUM EROSION DEPTH VS LEMDE NOZZLE ALTITUDE

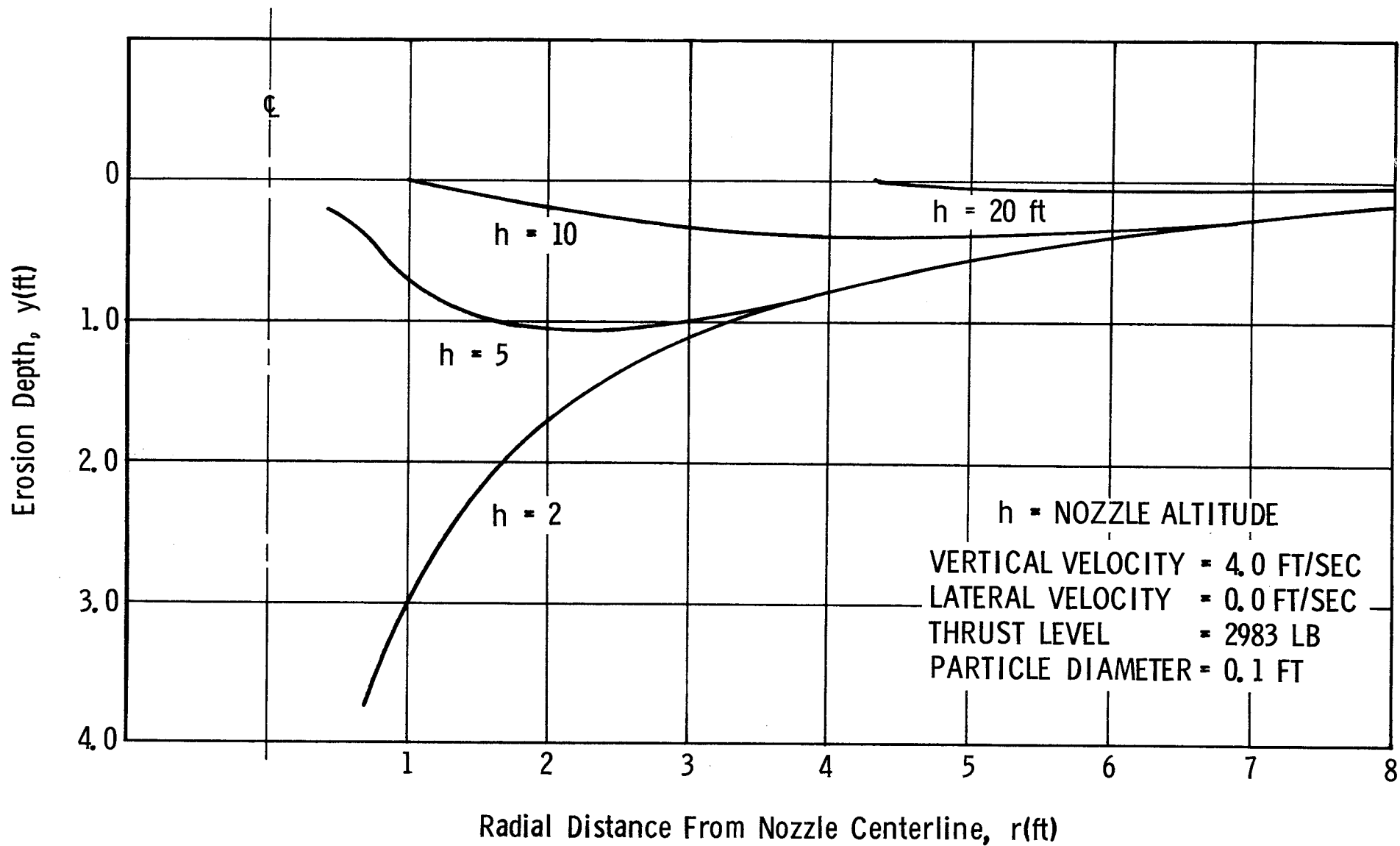


FIGURE 3 EROSION PROFILE DEVELOPMENT DURING A CONSTANT VELOCITY DESCENT FROM FORTY FEET

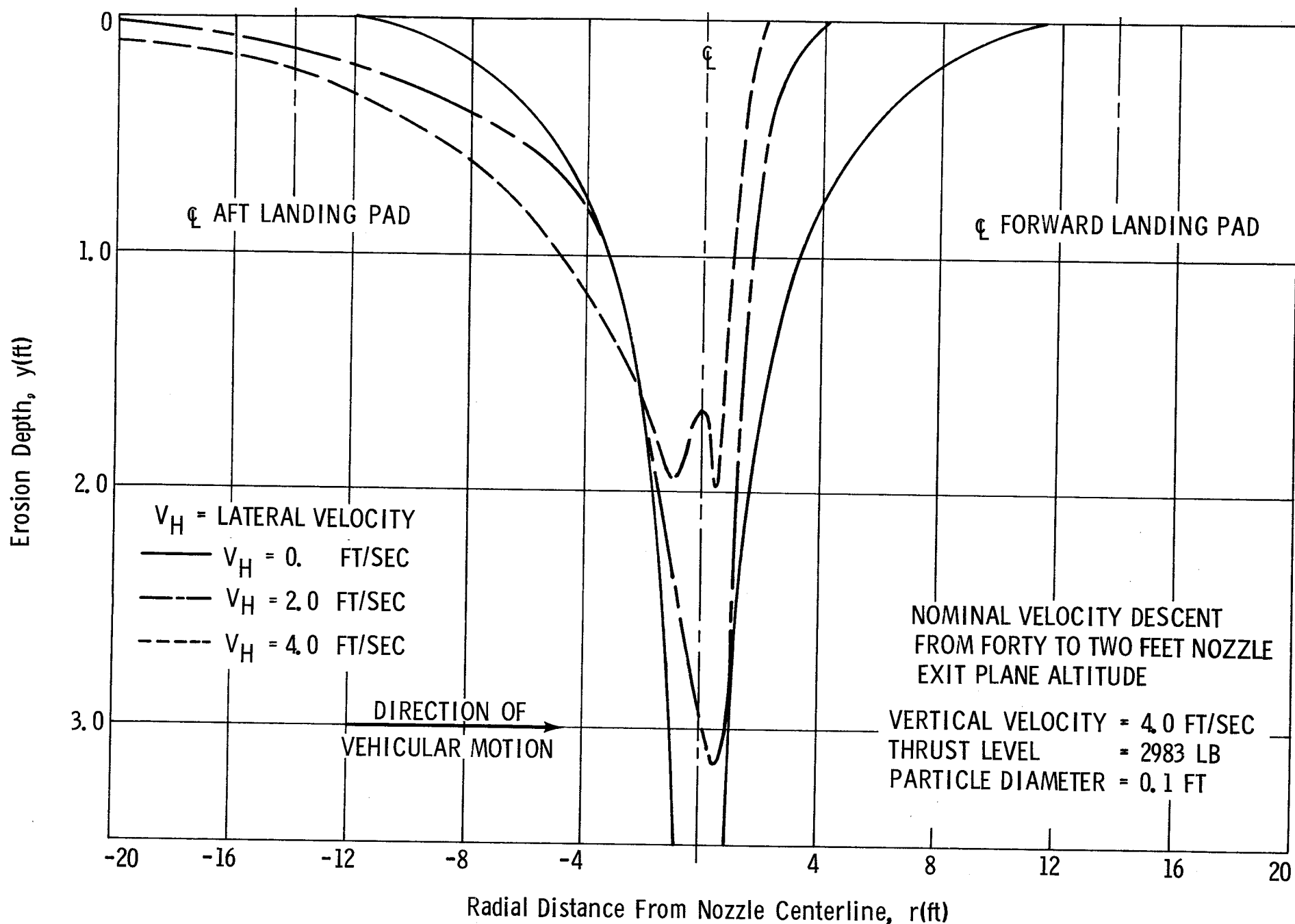


FIGURE 4 INFLUENCE OF THE HORIZONTAL VELOCITY COMPONENT UPON THE EROSION PROFILE

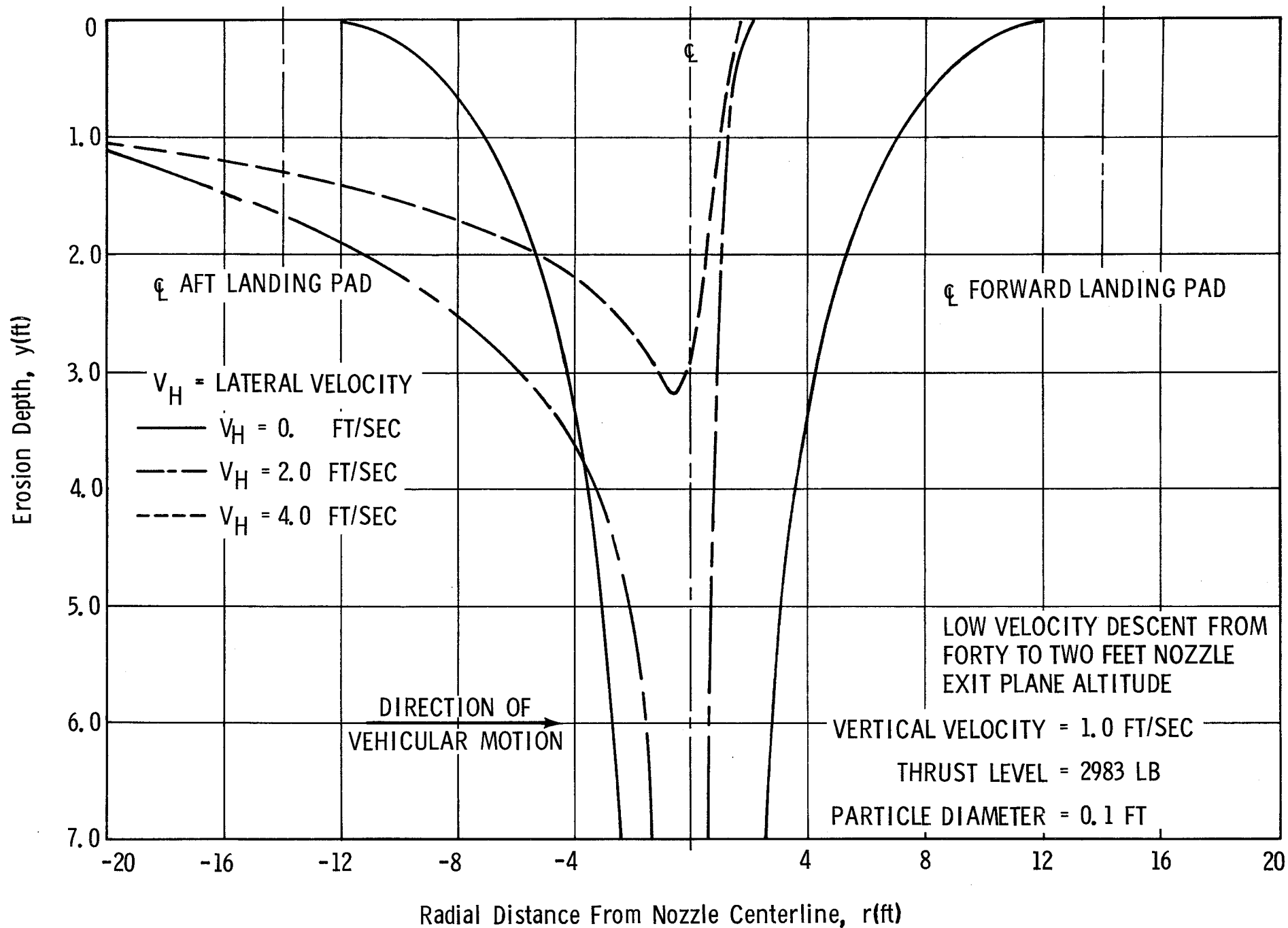


FIGURE 5 INFLUENCE OF THE HORIZONTAL VELOCITY COMPONENT UPON THE EROSION PROFILE

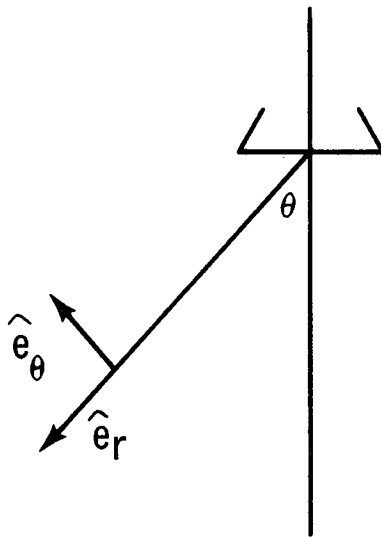


FIGURE 6

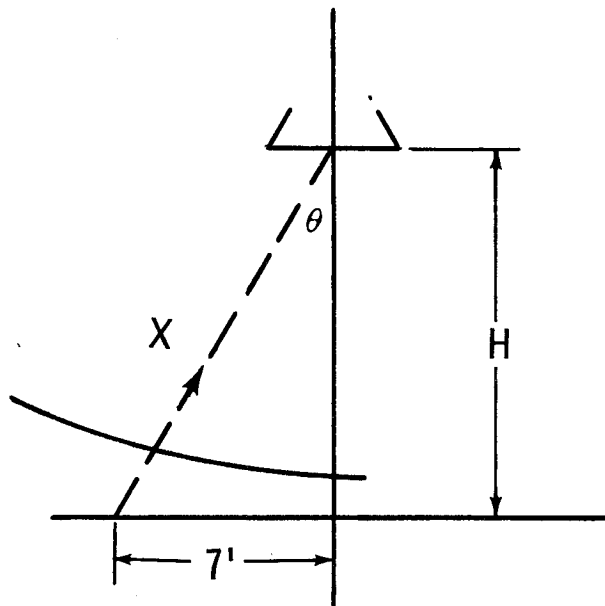


FIGURE 7

Distance Traveled Beyond Shock Wave (ft)

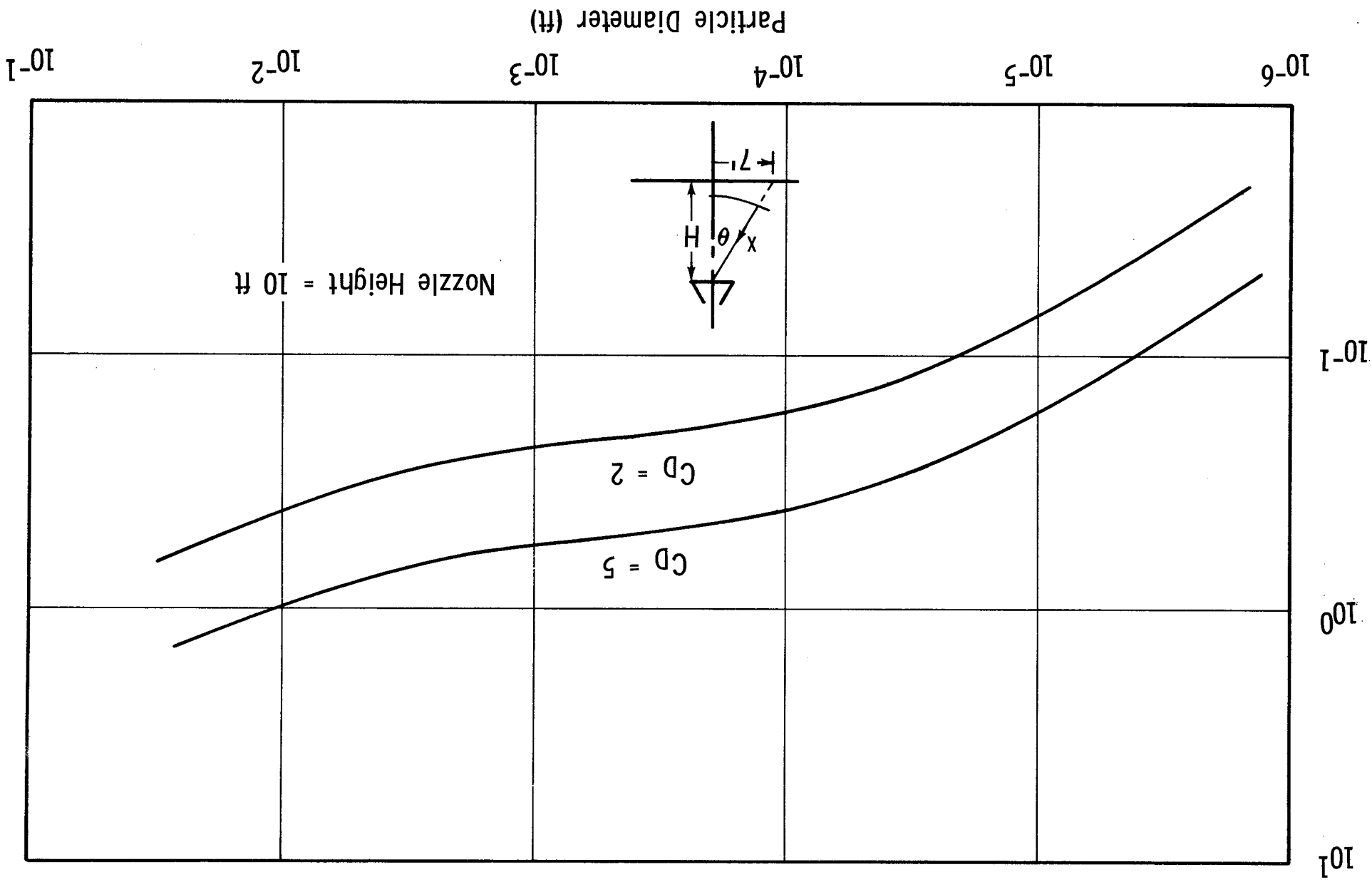


FIGURE 8 DISTANCE TRAVELED BEYOND SHOCK WAVE AS A FUNCTION OF PARTICLE DIAMETER

Distance Traveled Beyond Shock Wave (ft)

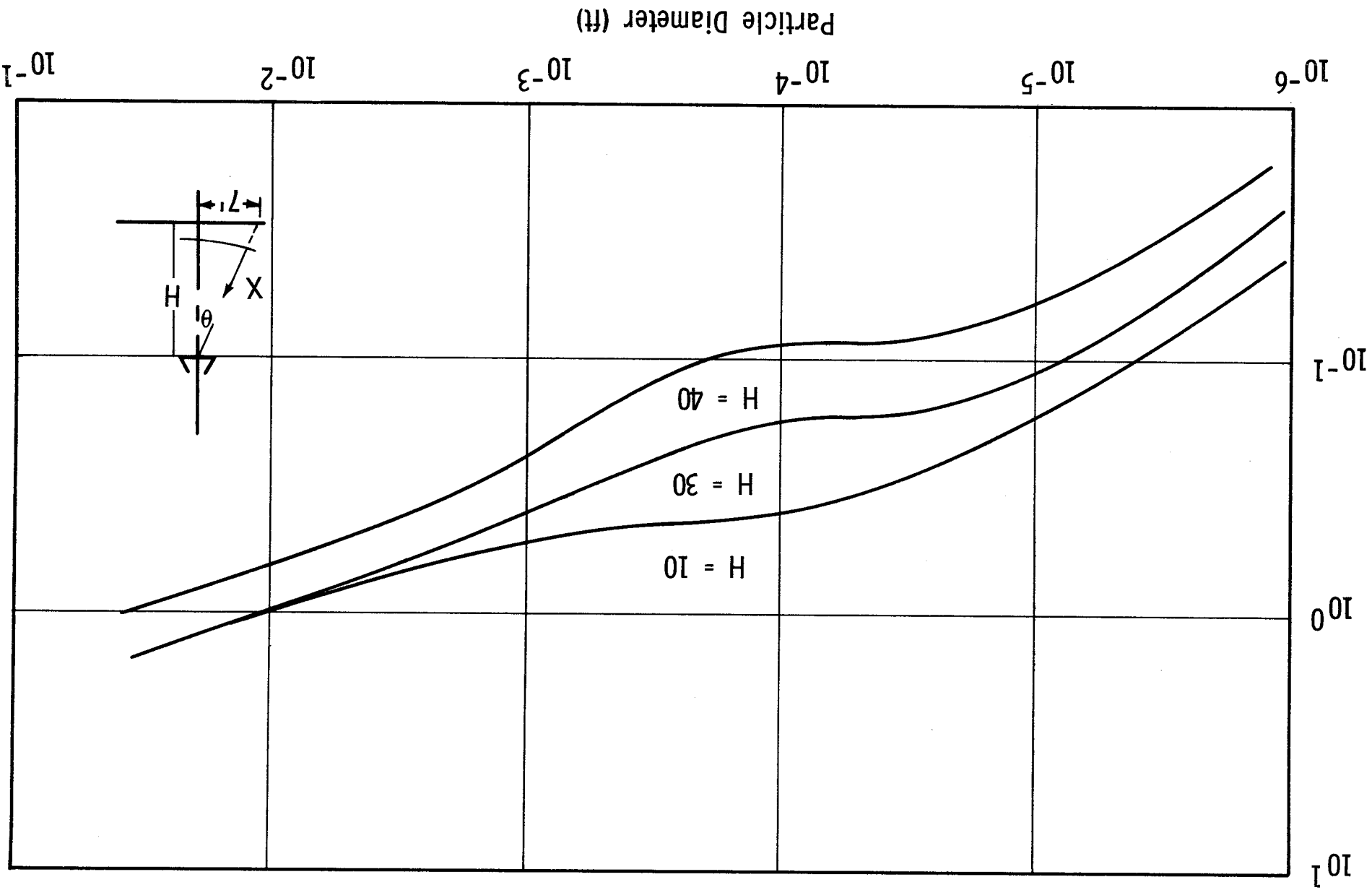


FIGURE 9 COMPARISON AS A FUNCTION OF PARTICLE DIAMETER BETWEEN DISTANCE TRAVELED BY PARTICLES TOWARD NOZZLE LOCATED AT VARIOUS HEIGHTS.

FIGURE 10 STAND-OFF DISTANCE - Δ (ft)
VS
VEHICLE HEIGHT - h (ft)

